Cancer Chemother Pharmacol (1992) 30: 86–94

Cancer Chemotherapy and Pharmacology

Toxicity and metabolism of 3′-deoxyadenosine N¹-oxide in mice and Ehrlich ascites tumor cells*

Karsten Ramløv Svendsen[1], Kay Overgaard-Hansen[1], Sune Frederiksen[2], Svend Aage Engelholm[3], Niels Tinggaard Pedersen[4], and Lars Lindhardt Vindeløv[3]

[1] Department of Biochemistry C and [2] Department of Biochemistry B, Panum Institute, University of Copenhagen, Copenhagen, Denmark
[3] Department of Oncology, Rigshospitalet, Copenhagen, Denmark
[4] Department of Pathology, Odense Hospital, Denmark

Received 23 January 1991/Accepted 23 January 1992

Summary. The toxic effect of 3′-deoxyadenosine N¹-oxide (3′-dANO) on mice, on their different organs, and on Ehrlich ascites tumor cells was studied. In both healthy and tumour-bearing animals, the lethal dose for 10% of the mice receiving i.p. injections (LD_{10}) of 3′-dANO was estimated to be about 300 mg/kg ×4 days in one mouse strain (Theiller). In another mouse strain (NMRI), we obtained a markedly higher LD_{10} value (675 mg/kg ×5 days). At nonlethal doses (250 mg/kg ×4 days), we observed reversible neurological symptoms on days 4–12 after treatment, but no macroscopical or microscopical changes was detected in the brain, heart, thymus, lung, lymph node, spleen, liver, kidney, bone marrow, or gastrointestinal tract. At doses of 450 mg/kg ×4 days, severe neurological symptoms were observed, and atony of the gastrointestinal canal and damage to the kidney and liver were registered. Even at doses that were lethal to the mice, no histopathological change was observed in the bone marrow or in the gastrointestinal canal. Pharmacokinetics studies showed that after the i.p. injection of 3′-dANO, the maximal plasma concentration was reached after 10 min, after which it declined showing a half-life of about 40 min. A transient accumulation of 3′-deoxyadenosine triphosphate (3′-dATP) was observed within 24 h in the liver and kidney, with the maximal concentration being reached after about 2–3 h. 3′-dANO was excreted partly as the unchanged substance and partly as the metabolite 3′-deoxyinosine within 24 h. Flow-cytometric DNA analysis of Ehrlich tumor cells treated either in vitro or in vivo with 3′-dANO revealed no therapy-induced change in the cell-cycle perturbations, which indicates that cells were randomly killed during all phases of the cycle.

* This work was supported by grants from the Director Ib Hendriksens Foundation and the P. Carl Petersens Foundation

Abbreviations: 3′-dANO, 3′-deoxyadenosine N¹-oxide; 3′-dA, 3′-deoxyadenosine; 3′-dI, 3′-deoxyinosine; 3′-dATP, 3′-deoxyadenosine triphosphate

Offprint request to: Kay Overgaard-Hansen, Department of Biochemistry B, Panum Institute, Blegdamsvej 3c, DK-2200 Denmark

Introduction

3′-Deoxyadenosine N¹-oxide (3′-dANO) is a synthetic derivative [14, 38] of the naturally occurring 3′-deoxyadenosine (3′-dA) [13]. The metabolism of 3′-dANO has been studied in Ehrlich cells in vitro [11, 38]. 3′-dANO is reduced to 3′-dA, which is either deaminated by adenosine deaminase (E.C. 3.5.4.4) to the inactive 3′-deoxyinosine (3′-dI) [12] or phosphorylated by adenosine kinase (E.C. 2.7.1.20) to 3′-deoxyadenosine monophosphate, which is further phosphorylated by adenylate kinase to 3′-deoxyadenosine triphosphate (3′-dATP) [25], which exerts a toxic effect due to its incorporation into RNA in lieu of ATP, thereby functioning as a chain terminator [27, 35].

3′-dA itself is an effective inhibitor of viral replication, an effect that is attributable to its ability to block polyadenylic acid [poly (A)] synthesis, and thus interferes with the processing and maturation of both cellular and viral mRNA [44]. In vivo, however, the effectiveness of 3′-dA as an antibacterial, antitumor, and antiviral agent is limited because of the rapid deamination of the compound to yield 3′-dI; the reaction is catalyzed by the widely distributed enzyme adenosine deaminase [1]. To overcome this problem in vivo, 3′-dA has been used in combination with inhibitors of adenosine deaminase such as 2′-deoxycoformycin [22].

3′-dANO has been shown to inhibit the growth of a variety of Ehrlich ascites tumor strains in mice [14, 38, 39]. The experiments indicate a correlation between the inhibition of tumor growth by 3′-dANO and the ability of the cell to form 3′-dATP from 3′-dANO and demonstrate that this conversion is determined by the rate of reduction of 3′-dANO (3′-dANO reductase activity) and by the ratio of the activity of adenosine kinase and that of adenosine deaminase in the cell. 3′-dANO is not a substrate for adenosine deaminase or adenosine kinase [28]. This indicates that 3′-dANO remains metabolically inert until it has entered a target cell that is capable of reducing 3′-dANO to 3′-dA. This observation is supported by in vivo investigations comparing the antitumor effects of 3′-dANO and 3′-dA

[13]. At equimolar doses, 3′-dANO exerts a markedly higher degree of tumor-growth inhibition than does 3′-dA.

The present report describes the general toxicity of 3′-dANO in whole mice and in their different organs. The effect of 3′-dANO on cell-cycle distribution in Ehrlich tumor cells was investigated, as was the metabolism and excretion of the substance in treated mice.

Materials and methods

3′-dANO was synthesized as described elsewhere [38]. [^{3}H]-3′-dANO (generally labeled) was prepared by Amersham (England). Five different lines of Ehrlich ascites tumor cells were transplanted into Theiller non-inbred mice [38]: the 3′-dANO-sensitive ELD and ELT cell lines and the 3′-dANO-insensitive Karolinska, New Klein, and Aarhus cell lines.

Toxicity of 3′-dANO. The toxicity of 3′-dANO in healthy Theiller mice was investigated as follows. Female mice weighing 25–30 g were injected i.p. with 450 mg/kg 3′-dANO daily for 4 days and, in another experiment, with 250 mg/kg daily for 4 days. Control mice received the same volume of 0.154 M NaCl i.p. Groups of two 3′-dANO-treated mice and one control mouse were anesthetized and autopsied at 2, 6, and 24 h and at 2, 3, 6, 8, 12, 20, and 27 days, respectively, after the last injection. The following organs were observed macroscopically and microscopically after samples had been stained with hematoxylin and eosin: the brain, thymus, lung, heart, lymph node, spleen, liver, kidney, bone marrow, and gastrointestinal tract.

Flow-cytometric DNA analysis. The flow cytometer used was a FACS III cell sorter. The tumor cells obtained for flow-cytometric DNA analysis were stored and prepared as previously described [41–43]. The DNA distribution was analyzed using a computer program that calculates the fractions of cells in the various cell-cycle phases [6]. The coefficient of variation (CV) for the G1 peak was calculated for all histograms and ranged from 2% to 4%.

The drug-induced influence on the cell-cycle distribution of Ehrlich ascites tumor cells was measured in vitro as well as in vivo by flow-cytometric DNA analysis. For in vitro analyses, tumor cells from the five different Ehrlich ascites tumors were harvested at 7 days after the i.p. injection of 0.2 ml undiluted ascites fluid into female mice. The cells were washed in phosphate-buffered saline and incubated with the drug as previously described [9]. Aliquots of 10^6 cells were continuously incubated with different concentrations of 3′-dANO on top of a layer of hardened agar (0.25%) in 35-mm petri dishes at 37° C in a humidified atmosphere of 5% CO_2 and 95% air. Aliquots of control cells were plated and incubated in the absence of drug as described above. The cells were harvested for flow-cytometric DNA analysis at 24 and 48 h after plating [9, 10].

For in vivo analyses, two experiments were performed using the 3′-dANO-sensitive ELT Ehrlich ascites tumor. In the first experiment, 20×10^6 cells were injected i.p. into female Theiller mice. On days 3–6 after inoculation, the mice received daily i.p. injections of 250 mg/kg 3′-dANO. Control mice received the sterile 0.154 M NaCl used as a solvent for 3′-dANO. In the treated group, three mice each were killed at 0, 4, 8, 12, 16, 20, 24, 36, 48, 72, and 96 h, respectively, after drug administration, and in the control group, three mice each were killed at 0, 12, 24, 36, 48, 72, and 96 h, respectively, after the injection of sterile 0.154 M NaCl. The tumor cells obtained from each mouse were harvested quantitatively, and samples were taken for cell counting and flow-cytometric DNA analysis [41–43]. In the second experiment, 20×10^6 cells were injected i.p. into female Theiller mice. At 3 days after inoculation, the mice received 3′-dANO every 4th h over a 24-h period at doses of 20, 40, and 60 mg/kg, respectively. Control mice received the same volume of sterile 0.154 M NaCl. Tumor cells for flow-cytometric DNA analysis were removed from the peritoneal cavity every 4th h over the same 24-h period by puncture with a hypodermic needle. The samples were handled as described for the first experiment.

Cell homogenates. Mouse livers and kidneys were minced with a scalpel and homogenized in a Potter-Elvehjem homogenizer with 4 times their weight of 50 mM sodium phosphate buffer (pH 7.2) at 4° C. Ehrlich tumor cells were washed with 0.154 M NaCl containing 1 mM ethylenediaminetetraacetic acid (EDTA, pH 7.4) and then suspended in 4 times their weight of 50 mM sodium phosphate buffer (pH 7.2) and lyzed by three freeze-thaw cycles in a bath at –80° C.

The 3′-dATP was determined in the neutralized acid-soluble fraction of cells after thin-layer chromatography (TLC) on cellulose plates in 1-propanol-H_2O-25% NH_4OH (30:5:15, by vol.) for 4 h to remove 3′-dANO and other nucleosides and bases from the application spot. The plates were then subjected to further chromatography for about 5 h in 0.32 M ammonium acetate/0.22 M lithium borate (pH 8.2) in 50% ethanol; in this solvent, the ribonucleotides form complexes with borate and remain at the original site, whereas 3′-deoxyadenosine mono-, di-, and triphosphate migrate [34]. The UV-absorbing spots of 3′-deoxyadenosine phosphates were eluted with water, and the concentration was calculated from the absorbance at 260 nm, assuming a molar absorbance coefficient of 15,000 M^{-1} cm^{-1}.

Determination of 3′-dANO, 3′-dI, and 3′-dA. To separate the 3′-deoxynucleosides from other purine bases, ribonucleosides, and nucleotides, the acid-soluble extracts were applied to PEI-cellulose TLC plates and chromatographed in 0.15% LiCl/1% boric acid. 3′-dANO and 3′-dI migrated in this solvent as one spot (R_f 0.9), and 3′-dA migrated with an R_f value of 0.7. The compounds were eluted with 0.02 M TRIS-HCl (pH 7.4) and were determined as follows:

1. 3′-dI was hydrolyzed in 0.5 M HCl at 100° C for 15 min. The solvent was neutralized and the formed hypoxanthine was determined enzymatically using xanthine oxidases (E.C. 1.2.3.2.) [23].

2. 3′-dA in the eluate was determined enzymatically using adenosine deaminase (E.C. 3.5.4.4.) [24].

3. 3′-dANO was determined by differential spectrophotometry. At pH 7.2, the spectrum of 3′-dANO exhibits a characteristic maximum at 233 nm, with the molar absorbance coefficient being 40,800 M^{-1} cm^{-1}. At pH zero (1 M HCl), the maximum at 233 nm switches to a minimum, with the molar absorbance coefficient being 4,300 M^{-1} cm^{-1}. The significant change from 40,800 to 4,300 in molar absorbance coefficients forms the basis for a sensitive assay of 3′-dANO. By diluting aliquots of a solution of 3′-dANO in either 0.02 M TRIS-HCl (pH 7.2) or 1 M HCl and measuring the absorbance at 233 nm, the concentration of 3′-dANO can be calculated from the difference in absorbance, the factor of dilution, and the differential molar absorbance coefficient of 36,500. Using this assay, 3′-dANO can be determined in mixtures with other compounds such as 3′-dA and 3′-dI, which do not give rise to changes in absorbance at 233 nm with the shift in pH. Likewise, this method enables the estimation of the 3′-dANO concentration in the acid-soluble extracts of plasma and liver.

Reduction of 3′-dANO in homogenates. The reduction of 3′-dANO was measured in a reaction mixture containing 50 mM sodium phosphate buffer (pH 7.2), 3.0 mM $MgCl_2$, 2.5 mM reduced nicotinamide adenine dinucleotide (NADH), 2.5 mM reduced nicotinamide adenine dinucleotide phosphate (NADPH), 6.0 mM glucose 6-phosphate 2 µg glucose 6-phosphate dehydrogenase from yeast (coenzyme NADH)/ml, 2 µg glucose 6-phosphate dehydrogenase from *Leuconostoc mesenteroides* (coenzyme NADPH)/ml, 3.0 mM 3′-dANO, and homogenate equivalent to 30–200 mg tissue (wet weight)/ml. Under these conditions, a constant rate of reduction was observed over 2 h. The incubation was performed at 37° C. Aliquots were taken over 2 h and deproteinized with perchloric acid, and the acid-soluble extract was neutralized with KOH. The reduction of 3′-dANO was followed either by measuring the disappearance of 3′-dANO from the acid-soluble extract using differential spectrophotometry or by measuring the amounts of 3′-dANO, 3′-dA, and 3′-dI after PEI-cellulose TLC chromatography and isolation of the compounds.

Enzyme assays. Cells were washed with 0.154 M NaCl containing 1 mM EDTA (pH 7.4), suspended in 4 times their weight of 20 mM TRIS-HCl buffer (pH 7.5) containing 1 mM dithiothreitol, and lyzed by three freeze-thaw cycles in a bath at –80° C. The lysate was used for enzyme assays

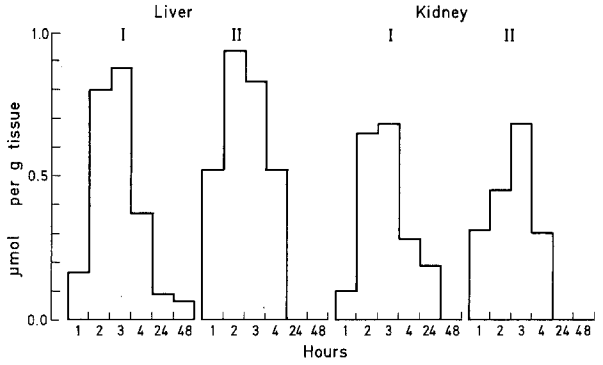

Fig. 1. Accumulation of 3′-deoxyadenosine phosphates in mouse livers and kidneys after the i.p. injection of 3′-dANO into 2 groups of 12 female mice each as follows: group I received 100 mg/kg 3′-dANO daily for 4 days, and group II was given one dose of 100 mg/kg 3′-dANO. Mice were killed at 1, 2, 3, 4, 24, and 48 h after the end of treatment, and the livers and kidneys were removed, weighed, and blended for 40 s with 4 times their weight of ice-cold perchloric acid (0.4 M). The amounts of 3′-deoxyadenosine mono-, di-, and triphosphate were determined in the acid-soluble fraction; 3′-dATP represented >90% of the total content of these phosphate esters. Each value represents the average of measurements made in 2 mice

after its dilution by 5–50 times with 20 mM TRIS-HCl buffer (pH 7.5) containing 0.5 mg bovine serum albumin/ml.

The adenosine deaminase assay (35 µl) used 50 mM TRIS-HCl buffer (pH 7.5), 1 mM EDTA, 3 mM dithiothreitol, 1.2 mM [U-^{14}C]-adenosine (1.75 mCi/mmol), and cell lysate equivalent to 0.2–1 mg cells (wet weight). The reaction mixture was incubated at 37° C, and five aliquots were taken during the 30-min incubation period and subjected to chromatography on PEI-cellulose TLC plates using a mixture of adenosine, inosine, and hypoxanthine as carriers. The TLC plates were developed for 3 h in 0.15% LiCl/1% boric acid. UV-absorbing spots were cut out and the radioactivity was determined.

The adenosine kinase assay (35 µl) comprised 90 mM TRIS-HCl buffer (pH 7.5), 1.0 mM $MgCl_2$, 2 mM dithiothreitol, 5 mM ATP, 0.3 µM 2′-deoxycoformycin, 30 µM [U-^{14}C]-adenosine (44 mCi/mmol), and cell lysate equivalent to 0.02–0.1 mg cells. The reaction mixture was incubated at 37° C, and five aliquots were taken during the 20-min incubation period and subjected to chromatography on PEI-cellulose TLC plates using adenosine and adenosine monophosphate (AMP) as carriers. The plates were developed for 3 h in 0.15% LiCl/1% boric acid. The adenosine spot and the adenine nucleotide spots were cut out and the radioactivity was determined. The kinase and deaminase reactions remained linear throughout the period of incubation.

Excretion of 3′-dANO and 3′-dI. Four female mice (24–26 g) were injected i.p. with 10 µmol 3′-dANO and placed in a metabolic cage (Techniplast, Italy) designed to collect urine and feces separately. Urine and feces were collected over 48 h. During the first 24 h, no food was given to the animals, but water was available ad libitum. The urine samples were heated to 100° C for 5 min and cooled in an ice bath, and a 1/6 vol of 3 M ice-cold perchloric acid was added. After centrifugation, the supernatant was neutralized with KOH. The feces samples were minced and extracted with 10 times their weight of H_2O at 100° C for 15 min. The samples were cooled in ice and centrifuged, and a 1/6 vol of 3 M perchloric acid was added to the supernatant. Following centrifugation, the supernatant was again neutralized. 3′-dANO, 3′-dA, and 3′-dI were isolated from the neutralized acid-soluble supernatants of urine and feces by two-dimensional TLC on PEI-cellulose TLC plates using H_2O in the first dimension and 0.15% LiCl/1% boric acid in the second. The compounds were eluted from the plates and determined as described above. The overall recovery achieved by these methods was 88%–90%.

Results

General toxicity

The toxicity of 3′-dANO to Theiller mice was evaluated from the following experiments. When healthy mice were injected i.p. with 450 mg/kg 3′-dANO daily for 4 days, 10 of 20 animals died, showing severe neurological symptoms characterized by balance disturbances and by a spin around their longitudinal axis. On treatment with 250 mg/kg for 4 days, 1 of 20 mice died, and reversible neurological symptoms such as those described above were observed from day 4 to day 12. In all experiments, the observation period was 30 days. In two experiments, mice were inoculated with Ehrlich ascites tumor cells and were then given i.p. injection of 400 mg/kg 3′-dANO on days 3–6 after transplantion; 4 of 12 mice died in one experiment and 3 of 11 died in the second study. As a rough estimate, in tumor-loaded mice, the LD_{10} value for 3′-dANO is around 300 mg/kg daily $\times 4$.

To clarify a possible difference in the toxicity of 3′-dANO to different mouse strains, we also chose to estimate the LD_{10} dose in the more frequently used NMRI strain. Groups of 18 healthy NMRI mice were injected i.p. with 3′-dANO for 5 days at daily doses of 200, 400, 500, 600, 700, 750, 775, and 800 mg/kg, i.v. injections were given at daily doses of 200, 300, 350, 400, and 500 mg/kg, and s.c. injections were given at daily doses of 400, 500, 600, 700, and 800 mg/kg. On the basis of this 5-day treatment schedule for NMRI mice, following an observation period of 30 days, the LD_{10} values for 3′-dANO were estimated to be 675 (i.p. injection), 320 (i.v. injection), and 475 mg/kg (s.c. injection).

Toxicity of 3′-dANO to organs

The effect of 3′-dANO on the different organs of mice was investigated after the i.p. injection of the drug at doses of 450 mg/kg daily in one series of animals and at daily doses of 250 mg/kg in a second series of 30 mice over 4 days. Autopsies following high-dose administration revealed atony of the gastrointestinal canal, necrosis and steatosis of the liver, atrophy and degeneration of the proximal tubules of the kidney, and depletion of lymphoblasts in the cortex of the thymus. In the low-dose series, no macroscopical or microscopical change was found in the brain, thymus, lung, heart, lymph node, spleen, liver, kidney, bone marrow, or gastrointestinal tract.

Metabolism of 3′-dANO in mice

The toxic effect exerted by 3′-dANO in different organs may be correlated to an accumulation of 3′-dATP. To test this possibility, we gave two groups of mice i.p. injections of 3′-dANO either daily at 100 mg/kg for 4 days or in a single dose of 100 mg/kg. After this treatment, two mice from each group were killed at different times and the content of 3′-deoxyadenosine mono-, di-, and triphosphate was determined in the livers and kidneys. The accumula-

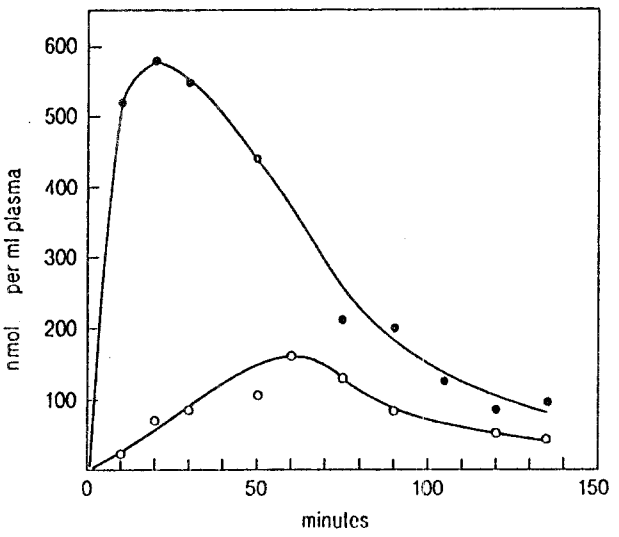

Fig. 2. Plasma levels of 3′-dANO and 3′-dI after the i.p. injection of a series of mice of uniform weight (22.5–23.0 g) with 3′-dANO (350 mg/kg). At different intervals after the injection the mice were killed by decapitation and the blood was collected. After centrifugation, a plasma sample was deproteinized with 1 vol 1 M perchloric acid, and the acid-soluble fraction was neutralized with KOH and analyzed for 3′-dANO (●) and 3′-dI (○)

Table 1. Content of 3′-deoxyadenosine phosphates, 3′-dANO, 3′-dA, and 3′-dI in mouse brain and blood after the injection of 3′-dANO

Tissue	Concentration (nmol/g tissue)			
	3′-deoxyadenosine phosphates	3′-dANO	3′-dI	3′-dA
Brain	3.2	<0.3	0.9	<0.3
Erythrocytes	22	0.9	1.4	<0.3
Plasma	0	1.4	2.3	<0.3

In all, 10.8 μmol [^{3}H]-3′-dANO in 0.154 M NaCl (sp. act., 142,000 dpm/nmol) was injected i.p. into a mouse weighing 40 g. After 3 h, the mouse was killed by decapitation and the blood was collected. The brain was removed, weighed, and homogenized with 2 vol ice-cold 0.4 M perchloric acid in a microblender. The cell volume of the erythrocytes was determined, and the cells and plasma were separated and deproteinized with 2 vol 0.4 M perchloric acid. The acid-soluble extracts were neutralized with KOH, and aliquots of the extracts were subjected to chromatography on PEI-cellulose TLC plates using a mixture of 3′-dATP, 3′-dANO, 3′-dI, and 3′-dA as carriers. The TLC plates were developed in *n*-butanol-water (86:18, v/v). The UV-absorbing spots were cut out and eluted with 0.7 M $MgCl_2$ in 0.02 M TRIS-HCl (pH 7.5). The radioactivity in the eluates was determined by liquid scintillation counting and corrected for quenching and counting efficiency. Each value represents the average of two determinations; 1 g erythrocytes is equivalent to 1 ml packed cells, and 1 ml plasma is assumed to weight 1 g

tion of 3′-deoxyadenosine phosphates is shown in Fig. 1. The amount of 3′-dATP represented >90% of the total content of these phosphate compounds. During the first 3 h after the end of treatment, the accumulation of about 0.9 μmol/g liver and 0.7 μmol/g kidney was observed in the two groups. During the following hour, the concentration of 3′-dATP decreased to about 50% in both groups, and after 24 h, no triphosphate could be detected in mice that had received one dose of 100 mg/kg. A prolonged clearance of 3′-dATP was observed in mice that had received this dose daily for 4 days. Following the administration of 3′-dANO at a higher dose (300 mg/kg) resulted in the same prolonged clearance pattern, but the maximal 3′-dATP concentrations measured were 2.5 μmol/g liver and 2.0 μmol/g kidney (data not shown).

The pattern of accumulation of 3′-dATP in the livers and kidneys of mice (Fig. 1) suggested that the concentration of 3′-dANO in the plasma must have been low after 2–3 h since no further accumulation took place in the organs after this time. Figure 2 shows the change in the plasma concentration of 3′-dANO after the i.p. injection of 350 mg/kg 3′-dANO. The maximal level was reached after 10–20 min, after which it decreased, showing a half-life of about 40 min. As a consequence of the reduction of 3′-dANO to 3′-dA in the different tissues, 3′-dA may be deaminated to 3′-dI, which then appears in the plasma. The changes in the levels of 3′-dI in plasma following the administration of 3′-dANO are also shown in Fig. 2. In this case, a transient accumulation of 3′-dI took place, with the peak concentration being reached after about 60 min.

To study the possible relationship between the neurological symptoms induced by 3′-dANO and the accumulation of 3′-deoxyadenosine phosphates or other metabolites of 3′-dANO in the brain, we gave a mouse an i.p. injection of 10.8 μmol [^{3}H]-3′-dANO. After 3 h, the mouse was killed, the brain was removed, and the blood was collected. 3′-Deoxyadenosine phosphates, 3′-dANO, 3′-dI, and 3′-dA were isolated and the radioactivity was measured. The results are presented in Table 1. Only marginal amounts of 3′-dANO and 3′-dA were detected in the brain, whereas significant levels of 3′-deoxyadenosine phosphates and 3′-dI were found. It should be taken into account, however, that the 5% blood content of the brain will increase these values, since the amount of 3′-deoxyadenosine phosphates and 3′-dI in the blood are several times higher than those in the brain. The accumulation of 3′-deoxyadenosine phosphates in the liver and kidney in situ (Fig. 1) shows that these tissues have a high capacity to reduce 3′-dANO to 3′-dA and to phosphorylate the latter to 3′-dATP. Further studies of these processes and of the enzymes involved were performed in cell homogenates.

Reduction of 3′-dANO in homogenates

The reduction of 3′-dANO to 3′-dA in homogenates of Ehrlich tumor cells and mouse liver proceeded in a non-linear fashion and leveled off within 15–30 min. However, following the addition of 2.5 mM NADH and NADPH, a constant rate of reduction was observed over 2 h. In the homogenates, 3′-dANO was converted to 3′-dI formed by the deamination of 3′-dA, and no further degradation of 3′-dI was observed.

The activities of 3′-dANO reductase, adenosine kinase, and adenosine deaminase in homogenates of mouse liver and mouse kidney were compared with the enzyme activi-

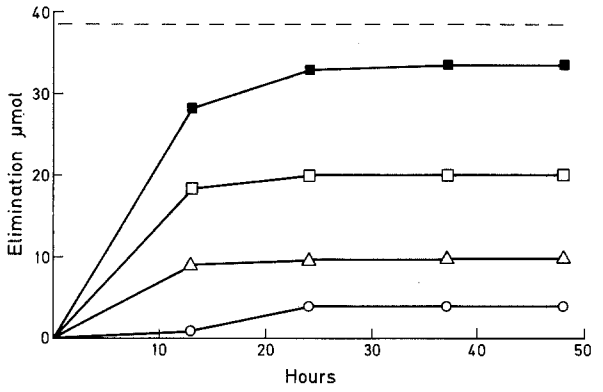

Fig. 3. Excretion of 3′-dANO and 3′-dI in the urine and feces of mice. Each of 4 female mice (24–26 g) was injected i.p. with 9.9 µmol 3′-dANO, and samples of urine and feces were collected during the first 48 h after treatment and analyzed for 3′-dANO and 3′-dI. ○, 3′-dI in feces; △, 3′-dI in urine; □, 3′-dANO in urine; ■, sum of 3′-dANO and 3′-dI in urine and feces; *dotted line,* total amount of 3′-dANO injected. Each point represents the sum of the respective amount of nucleosides found in the 4 mice.

Table 2. Activity of 3′-dANO reductase, adenosine kinase, and adenosine deaminase in homogenates of mouse liver, mouse kidney, and 3′-dANO-sensitive and resistant Ehrlich ascites tumor cells

Homogenates	Enzyme activity (nmol h^{-1} mg $cells^{-1}$)			
	3′-dANO reductase	Adenosine kinase	Adenosine deaminase	Ratio of kinase/ deaminase
Liver	14.4	250	70	3.6
Kidney	7	30	55	0.55
Ehrlich cells ELT, 3′-dANO-sensitive)	1.4	30	11	2.7
Ehrlich cells (Aarhus, 3′-dANO-resistant)	1.1	13	83	0.16

Enzyme activities were determined as described in Materials and methods. Each value represents the average of two determinations that differed by no more than 10%

ties in 3′-dANO-resistant and sensitive Ehrlich ascites tumor cells (Table 2). The 3′-dANO reductase activity in the liver and kidney was 5–10 times higher than that in Ehrlich cells. The activity of adenosine deaminase was 5–6 times higher in the liver and kidney than it was in 3′-dANO-sensitive Ehrlich cells, but the adenosine kinase activity was up to 8 times higher in the organ homogenates. The ratio of adenosine kinase/adenosine deaminase activity and the relatively high reduction capacity are in good agreement with the marked accumulation of 3′-deoxyadenosine phosphates observed in these tissues (Fig. 1).

Excretion of 3′-dANO and 3′-dI

The excretion of 3′-dANO and 3′-dI in the urine and feces were measured in four mice treated i.p. with 100 mg/kg 3′-dANO (Fig. 3). Within the first 12 h after the injection

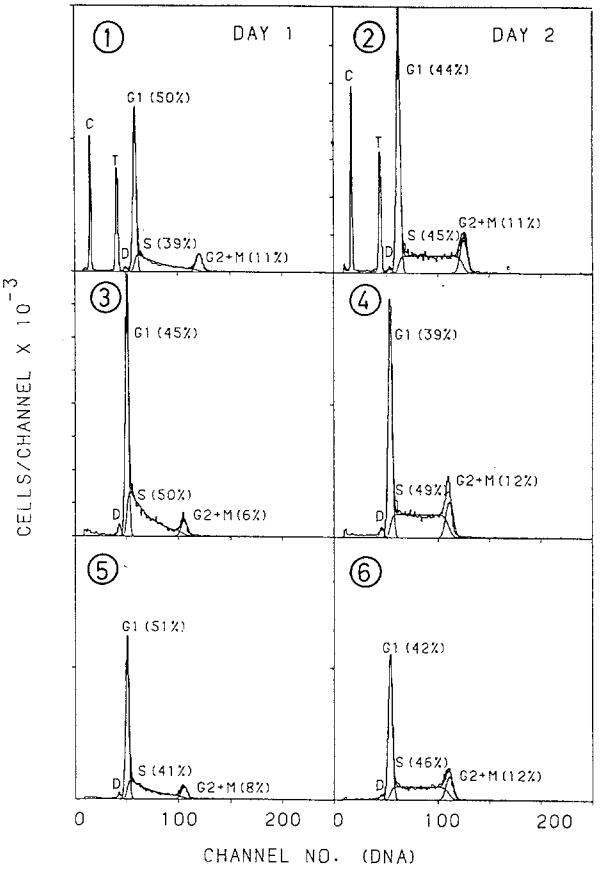

Fig. 4. Flow-cytometric DNA histograms obtained after the exposure of Ehrlich ascites tumor cells ELT to 3′-dANO. The fractions of cells in the different cell-cycle phases are given in parentheses. *C* and *T* represent the internal standards (chicken and trout erythrocytes) used to calculate the DNA index, and peaks marked *D* represent normal murine stromal cells. *1, 2,* controls on days 1 and 2; *3, 4,* incubation with 14 µM 3′-dANO on days 1 and 2; *5, 6,* incubation with 140 µM 3′-dANO on days 1 and 2

of 3′-dANO, 50% of the drug was recovered unchanged in the urine and 25% was excreted in the form of 3′-dI. In feces, 10% of the parent drug was excreted as 3′-dI at 12–24 h after 3′-dANO injection, whereas no 3′-dANO could be detected. After 24 h, the total recovery was close to 85%. Taking into account that the recovery of 3′-dANO and 3′-dI that had been added to fresh urine was 88%–90%, it is reasonable to conclude that all of the 3′-dANO given at moderate doses such as that above was excreted either unchanged or as 3′-dI within 24 h.

Effect of 3′-dANO on cell-cycle distribution

The influence of 3′-dANO on the cell-cycle distribution of Ehrlich ascites cells was measured in vitro as well as in vivo. Two 3′-dANO-sensitive Ehrlich cell lines (ELT and ELD) and three resistant cell lines (New Klein, Aarhus, and Karolinska) [38] were treated with concentrations of 1.4×10^{-2}, 1.4×10^{-1}, 1.4, 14, 1.4×10^{2} and 1.4×10^{3} µM 3′-dANO. No significant cell-cycle change was detected after in vitro incubation with 3′-dANO in either the re-

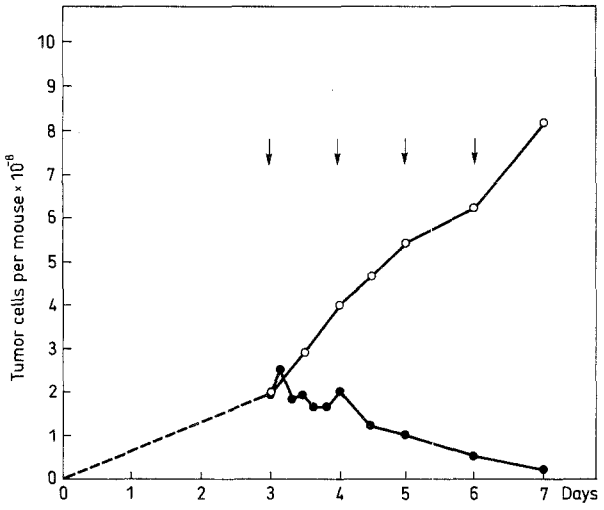

Fig. 5. 3′-dANO-inhibition pattern of Ehrlich ascites cells ELT grown in vivo for flow-cytometric DNA analysis. In all, 20×10^6 Ehrlich ascites cells ELT were injected into a group of female Theiller mice. On days 3–6 after inoculation, the mice received daily i.p. injections of 250 mg/kg 3′-dANO. Control mice received the 0.154-M NaCl used as a solvent for 3′-dANO. The treated mice were killed at 0, 4, 8, 12, 16, 20, 24, 36, 48, 72, and 96 h after the injection, respectively; Control animals were killed at 0, 12, 24, 36, 48, 72, and 96 h after treatment. Cell samples were taken from each mouse for cell counting and flow-cytometric DNA analysis. Each point represents the average number of tumor cells found in the peritoneal cavities of 3 mice. *Arrows* mark the time of injection of the drug. ○, Control mice; ●, 3′-dANO-treated mice

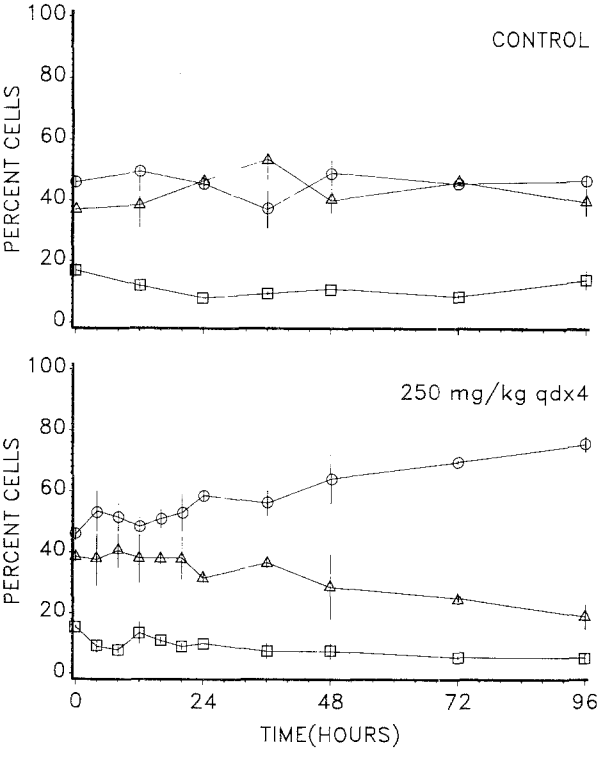

Fig. 6. Cell-cycle distribution of Ehrlich ascites cells ELT treated in vivo with 3′-dANO. Cell samples obtained in the experiment described in the legend to Fig. 5 were analyzed by flow-cytometric DNA analysis. △, G_1 phase; ○, S phase; □, G_2 +M phase

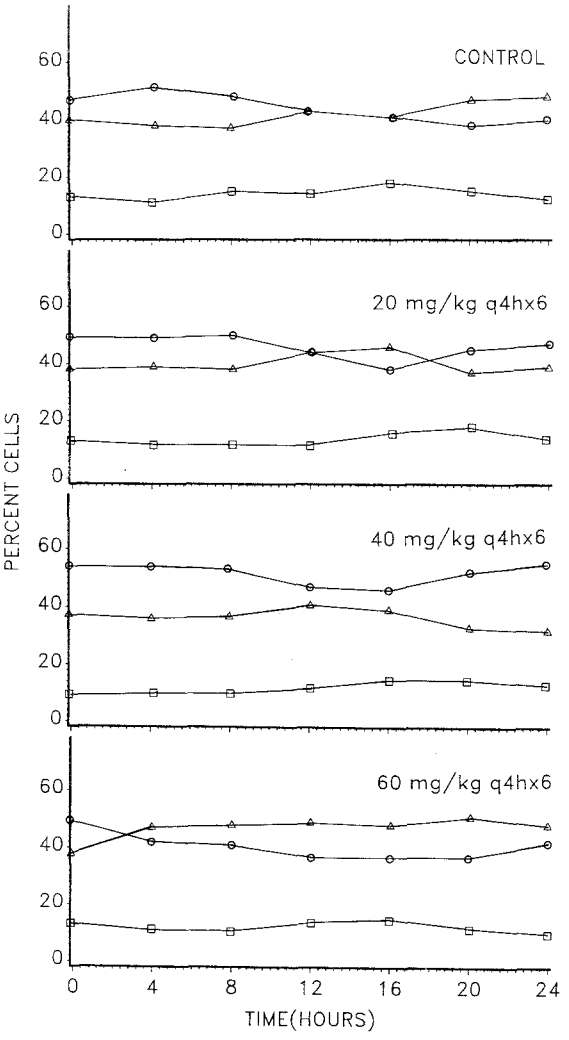

Fig. 7. Cell-cycle distribution of Ehrlich ascites cells ELT treated in vivo every 4th h with multiple doses of 3′-dANO. At 4 days after inoculation, the mice received 3′-dANO every 4th h over a 24-h period at doses of 20, 40, and 60 mg/kg, respectively. Tumor cells for flow-cytometric DNA analysis were removed from the peritoneal cavity every 4th h over the same period. △, G_1 phase; ○, S phase; □, G_2+M phase

sistant or the sensitive tumor cells. The results obtained using the sensitive ELT cell line are shown in Fig. 4. When ELD or ELT cells were grown for 24 h in RPMI medium supplemented with 10% fetal calf serum in the presence of 140 and 375 μM 3′-dANO, their growth was inhibited by 50% and 95%, respectively.

Flow-cytometric DNA analysis was also performed on sensitive ELT tumor cells obtained directly from 3′-dANO-treated mice. Each mouse received 250 mg/kg 3′-dANO on days 3–6 after tumor-cell inoculation. At different intervals after drug administration, three mice were killed, the tumor cells from each mouse were harvested quantitatively, and samples were taken for cell counting and flow-cytometric DNA analysis. Figure 5 shows the cell numbers found vs time in 3′-dANO-treated and control mice. The cell numbers in the treated mice remained constant from day 3 to day 4 and then decreased to nearly zero values on day 7.

Figure 6 shows the changes in the cell-cycle distribution during 3′-dANO treatment as determined by flow-cytometric DNA analysis. No change was apparent during the first 24 h after the start of the treatment. Subsequently, we observed a gradual decrease in the G1 fraction and an increase in the S fraction over the interval between 24 and 96 h. To study any possible acute effects on cell-cycle distribution, we performed another experiment. At 4 days after tumor-cell inoculation, 3′-dANO was injected into mice at doses of 20–60 mg/kg every 4 h over a 24-h period. Cell samples were taken from the peritoneal cavity every 4th h for flow-cytometric DNA analysis (Fig. 7). Even on this frequent schedule of administration of high-dose 3′-dANO, no obvious change in the cell-cycle distribution occurred within the 24-h observation period.

Discussion

3′-dANO inhibits tumor growth in some mouse-derived tumors [14, 38, 39], and its inhibitory activity is stronger than that exerted by 3′-dA at equimolar doses [14]. The advantage of using 3′-dANO in vivo is that the drug is not reduced to 3′-dA in the circulatory system and thus is not metabolized until it reaches the target cell [38, 39].

We determined the lethal dose of 3′-dANO in two different mouse strains and observed a marked discrepancy in toxicity. The LD_{10} value found for the NMRI strain was >2-fold that determined for the Theiller strain. This finding might be explained by either a higher level of degradation enzymes in the liver or a higher rate of 3′-dANO excretion in the kidneys of NMRI mice. No essential difference in the general toxicity of 3′-dANO was found between healthy mice and tumor-bearing animals. A different situation exists for 3′-dA in that the tolerable dose appears to vary between healthy and tumor-bearing mice (300 and 200 mg/kg ×7 days, respectively) [21]. The LD_{10} value for 3′-dANO in tumor-bearing mice was estimated in our investigations to be about 300 mg/kg ×4 days.

It is noteworthy that no toxic effect was produced by 3′-dANO in the bone marrow or in the mucosa of the gastrointestinal canal, even at LD_{50} doses. The atony that developed in the gastrointestinal tract after high-dose administration was probably related to the neurotoxic action of the drug. The lack of effect of 3′-dANO in the majority of organs may be due to the inability of the latter to form 3′-dATP due either to a reduced capacity to convert 3′-dANO to 3′-dA or to a low ratio of adenosine kinase/adenosine deaminase activity. The latter possibility is supported by the observation that this ratio in the mouse jejunum is extremely low (0.018), primarily due to the extremely high activity of adenosine deaminase [2]. The relatively severe damage seen in the liver after high-dose 3′-dANO treatment is therefore most likely caused by the high capacity of this organ to convert 3′-dANO to 3′-dATP (Fig. 1). The kinase and deaminase activities determined in the liver in the present study (Table 2) support this conclusion and are in agreement with previously reported data [2].

Bear et al. [4] demonstrated that 3′-dA inhibited acetylcholinesterase activity in mouse neuroblastoma cells, and both the rate and the extent of neurite formation were depressed [4]. These findings might partially explain the observed neurotoxicity. Moreover, adenosine is a major neuromodulator of CNS function [29, 36]. Adenosine and several of its analogues depress the activity of the CNS, partly by inhibiting transmitter release [8, 16]. One of the highest-density receptor sites lies in the molecular layer of the cerebellum [17]; 3′-dANO may have a direct effect on these receptors and thereby give rise to the neurological symptoms observed, but this hypothesis must be tested in further experiments.

The cytostatic effect of both 3′-dA and 3′-dANO is correlated to their conversion to 3′-dATP in the cell. The toxic effect of 3′-dATP is assumed to involve the inhibition of RNA synthesis via incorporation of the triphosphate into the growing RNA chains in lieu of ATP, resulting in chain termination [27, 35]. The inhibitory effect of 3′-dA on the synthesis of ribosomal RNA [40], low-molecular-weight RNA [15], polyadenylic acid [7, 30], and mRNA [3] are well documented. 3′-dATP is not incorporated into DNA [37], but 3′-dA inhibits ^{32}P incorporation into both RNA and DNA [26]. This inhibition is attributable to the inhibitory effect of 3′-dATP on the formation of 5-phosphoribosyl-1-pyrophosphate from ribose-5-phosphate [31].

The effect of 3′-dANO on the cell-cycle distribution of Ehrlich ascites tumor cells was measured by flow-cytometric DNA analysis [19]. No cell-cycle change was detected after 48 h incubation in vitro (Fig. 4). The effect of 3′-dANO on the cell-cycle distribution was also studied in vivo by sequential DNA analysis of tumor cells following the treatment of mice with 3′-dANO. No change was seen during the first 24 h after the start of treatment, but we subsequently observed a gradual decrease in the G1 fraction and an increase in the S fraction (Fig. 6). It should be noted that concurrent with these changes in the cell cycle, a decrease in cell number amounting to nearly two decades took place (Fig. 5). We could not determine with certainty whether the cell-cycle changes were caused by a blocking of the cells in the S phase by the drug by a selective loss of cells from the other phases, or by a combination of these mechanisms. Likewise, when 3′-dANO was given every 4 h over the first 24 h at doses of 20–60 mg/kg, no apparent effect on the cell distribution was observed (Fig. 7). An acute effect of the drug on the cell-cycle distribution could thus be excluded. The conclusion to be drawn from these results is that 3′-dANO exerts its cytostatic action without perturbing the cell cycle and that only as the cells are dying and disappearing does an increase in the S phase occur among the remaining cells. This conclusion is in good agreement with the known action of 3′-dA as on RNA inhibitor that does not suppress DNA synthesis.

Other adenosine analogues have been investigated with regard to the relationship between their cytotoxicity and their effect on cell-cycle distribution. Adenosyl homocysteinase in L1210 leukemia cells was more strongly inhibited by 9-β-D-arabinofuranosyladenine (ara-A) than by 3′-dA [5]. At high concentrations, there was no apparent difference in the cytotoxicity of ara-A to synchronous HeLa cells between the G1 and the mid-S phase, suggesting that the drug is not strongly phase-specific. Unlike 3′-dANO, the deoxyadenosine analogues 2-chloro-2′-

deoxyadenosine and 2-bromo-2′-deoxyadenosine cause an accumulation of CCRF-CEM cells in the S phase [20]; at higher doses, these agents block cells at the G1-S transition [20, 32, 33]. These findings can be explained by the inhibitory effect of 2-chloro-2′-deoxyadenosine and 2-bromo-2′-deoxyadenosine on DNA synthesis [18, 20, 32].

However, recent findings have shown that 3′-dATP has a profound effect on the cytoskeleton structure of both interphase and dividing cells [45, 46]. In cultures of fibroblast and epidermal cells, the addition of 3′-dA gave rise to a rapid accumulation of 3′-dATP. Under such conditions, it was observed that the intermediate filament arrays in interphase cells collapsed into perinuclear caps and that dividing cells were arrested at the onset of mitosis, showing depolymerization of the microtubules to small asters. These findings suggest that the effect of 3′-dATP may be fatal to the cell at any stage of the cell cycle. This view is supported by the present results, which demonstrate evenly distributed cell killing by 3′-dANO during all phases of the cell cycle. Due to its mode of action, 3′-dANO might be valuable as an antitumor agent, especially in combination with drugs whose action is primarily exerted against the synthesis of DNA.

Acknowledgements. We thank Ms. C. Goos Iversen, Ms. K. Samuelsen and Ms. R. Jensen for their excellent technical assistance.

References

1. Agarwal RP, Sagar SM, Parks RE (1975) Adenosine deaminase from human erythrocytes: purification and effects of adenosine analogs. Biochem Pharmacol 24: 693–701
2. Arch JRS, Newsholme EA (1978) Activities and some properties of 5′-nucleotidase, adenosine kinase and adenosine deaminase in tissues from vertebrates and invertebrates in relation to the control of the concentration and the physiological role of adenosine. Biochem J 174: 965–977
3. Beach LR, Ross J (1978) Cordycepin. An inhibitor of newly synthesized globin messenger RNA. J Biol Chem 253: 2628–2632
4. Bear MP, Schneider FH (1979) The effects of actinomycin D and cordycepin on neurite formation and acetylcholinesterase activity in mouse neuroblastoma cells. Exp Cell Res 123: 301–309
5. Cass CF, Selner M, Ferguson PJ, Phillips JR (1982) Effects of 2′-deoxyadenosine, α, β-D-arabinofuranosyladenine, and related compounds on S-adenosyl-L-homocysteine hydrolase activity in synchronous and asynchronous cultured cells. Cancer Res 42: 4991–4998
6. Christensen I, Hartmann NR, Keiding N, Larsen JK (1978) Distribution from cell populations with partial synchrony. In: Lutz D (eds) Pulse-cytophotometry, vol 3. European Press, Ghent, pp 71–78
7. Darnell JE, Philipson L, Wall R, Adesnik M (1971) Polyadenylic acid sequences: role in conversion of nuclear RNA into messenger RNA. Science 174: 507–510
8. Dunwiddie TV (1985) The physiological role of adenosine in the central nervous system. Int Rev Neurobiol 27: 63–139
9. Engelholm SA, Spang-Thomsen M, Vindeløv LL (1983) A short-term in vitro test for tumor sensitivity to Adriamycin based on flow cytometric DNA analysis. Br J Cancer 47: 497–502
10. Engelholm SA, Spang-Thomsen M, Vindeløv LL, Brünner N (1986) Chemosensitivity of human small cell carcinoma of the lung detected by flow cytometric DNA analysis of drug-induced cell cycle perturbations in vitro. Cytometry 7: 243–250
11. Frederiksen S (1963) Inhibition of ribonucleic acid and deoxyribonucleic acid synthesis in Ehrlich ascites cells by cordycepin-N^1-oxide. Biochim Biophys Acta 76: 366–371
12. Frederiksen S (1966) Specificity of adenosine deaminase towards adenosine and 2′-deoxyadenosine analogues. Arch Biochem Biophys 113: 383–388
13. Frederiksen S, Klenow H (1975) 3′-Deoxyadenosine and other polynucleotide chain terminators. In: Sartorelli AC, Johns OG (eds) Handbook of experimental pharmacology. Springer, Berlin Heidelberg New York, pp 657–659
14. Frederiksen S, Rasmussen AH (1967) Effect of the N^1-oxides of adenosine,2′-deoxyadenosine and 3′-deoxyadenosine on tumor growth in vivo. Cancer Res 27: 385–391
15. Frederiksen S, Pedersen IR, Hellung-Larsen P, Engberg J (1974) Metabolic studies of small molecular weight nuclear RNA components in BHK 21 cells. Biochim Biophys Acta 340: 64–76
16. Fredholm BB, Hedqvist P (1980) Modulation of neurotransmission by purine nucleosides and nucleotides. Biochem Pharmacol 29: 1635–1643
17. Goodmann RR, Snyder SH (1982) Autoradiographic localization of adenosine receptors in rat brain using [^{3}H]-cyclohexyladenosine. J Neurosci 2: 1230–1241
18. Griffig J, Koob R, Blakley RL (1989) Mechanisms of inhibition of DNA synthesis by 2-chlorodeoxyadenosine in human lymphoblastic cells. Cancer Res 49: 6923–6928
19. Hill B, Whelan H, Rupiniate HT, Dennis LY, Rosholt MA (1981) A comparative assessment of the in vitro effect on cells by means of colony assays or flow microfluourimetry. Cancer Chemother Pharmacol 7: 21–26
20. Huang MC, Ashmun RA, Avery TL, Kuehl M, Blakley RL (1986) Effects of cytotoxicity of 2′-deoxyadenosine and 2-bromo-2′-deoxyadenosine on cell growth, clonogenicity, DNA synthesis, and cell cycle kinetics. Cancer Res 46: 2362–2368
21. Jagger DV, Kredich NM, Guarino AJ (1961) Inhibition of Ehrlich mouse ascites tumor growth by cordycepin. Cancer Res 21: 216–220
22. Johns DG, Adamson RH (1976) Enhancement of the biological activity of cordycepin (3′-deoxyadenosine) by the adenosine deaminase inhibitor 2′-deoxycoformycin. Biochem Pharmacol 25: 1441–1444
23. Kalckar HM (1947) Differential spectrophotometry of purine compounds by means of specific enzymes. J Biol Chem 167: 429–444
24. Kalckar HM (1947) Differential spectrophotometry of purine compounds by means of specific enzymes: II. Determinations of adenine compounds. J Biol Chem 167: 445–459
25. Klenow H (1963) Formation of the mono-, di-, and triphosphate of cordycepin in Ehrlich ascites tumor cells in vitro. Biochim Biophys Acta 76: 347–353
26. Klenow H (1963) Inhibition by cordycepin and 2-deoxyglucose of the incorporation of [^{32}P]-orthophosphate into the nucleic acids of Ehrlich ascites tumor cells in vitro. Biochim Biophys Acta 76: 354–365
27. Klenow H, Frederiksen S (1964) Effect of 3′-deoxy ATP (cordycepintriphosphate) and 2′-deoxy ATP on the DNA-dependent RNA nucleotidyltransferase from Ehrlich ascites tumor cells. Biochim Biophys Acta 87: 495–498
28. Lindberg B, Klenow H, Hansen K (1967) Some properties of partially purified mammalian adenosine kinase. J Biol Chem 242: 350–356
29. Marangos PJ, Boulanger JP (1985) Basic and clinical aspects of adenosinegic neuromodulation. Neurosci Biobehav Rev 9: 421–430
30. Mendecki J, Lee SY, Brawerman G (1972) Characteristics of the polyadenylic acid segment associated with messenger ribonucleic acid in mouse sarcoma 180 ascites cells. Biochemistry 11: 792–798
31. Overgaard-Hansen K (1964) The inhibition of 5-phosphoribosyl-1-pyrophosphate formation by cordycepin triphosphate in extracts of Ehrlich ascites tumor cells. Biochim Biophys Acta 80: 504–507
32. Parsons PG, Bowman EP, Blakley RL (1986) Selective toxicity of deoxyadenosine analogues in human melanoma cell lines. Biochem Pharmacol 35: 4025–4029
33. Pemble LB, Lihou MG, Blakey RL, Jamieson GP, Smith PJ (1987) Lack of cross-resistance between cytosine arabinoside and a new halogenated nucleoside analogue, 2-bromo-2′-deoxyadenosine in

human acute myeloid leukaemia cells. Cancer Chemother Pharmacol 20: 155–161
34. Plesner PE (1955) Methods for studying nucleotide metabolism in synchronized cultures of protozoa. Acta Chem Scand [B] 9: 197
35. Shigeura HT, Boxer GE (1964) Incorporation of 3′-deoxyadenosine 5′-triphosphate into RNA by polymerase from *Micrococcus lysodeikticus*. Biochem Biophys Res Commun 17: 758–763
36. Snyder SH (1985) Adenosine as a neuromodulator. Annu Rev Neurosci 8: 103–124
37. Suhadolnik RJ (1970) Nucleoside antibiotics. Wiley-Interscience, New York, p 62
38. Svendsen KR, Overgaard-Hansen K, Frederiksen S, Loft H, Engelholm SA (1987) Studies on the mechanism of cytotoxicity of 3′-deoxyadenosine N^1-oxide in different strains of Ehrlich ascites tumor cells. Cancer Chemother Pharmacol 19: 118–122
39. Svendsen KR, Overgaard-Hansen K, Frederiksen S (1988) Synergistic effect of 3′-deoxyadenosine N^1-oxide and adenosine deaminase inhibitors on growth of Ehrlich ascites tumor cells in vivo. Cancer Chemother Pharmacol 21: 35–39
40. Truman JT, Frederiksen S (1969) Effect of 3′-deoxyadenosine and 3′-amino-3′-deoxyadenosine on the labelling of RNA sub-species in Ehrlich ascites tumor cells. Biochim Biophys Acta 182: 36–45
41. Vindeløv LL, Christensen IJ, Keiding N, Spang-Thomsen M, Nissen NI (1983) Long-term storage of samples for flow cytometry DNA analysis. Cytometry 3: 317–322
42. Vindeløv LL, Christensen IJ, Nissen NI (1983) A detergent-trypsin method for the preparation of nuclei for flow cytometric DNA analysis. Cytometry 3: 323–327
43. Vindeløv LL, Christensen IJ, Nissen NI (1983) Standard deviation of high-resolution flow cytometric DNA analysis by simultaneous use of chicken and trout red blood cells as internal reference standards. Cytometry 3: 328–331
44. Wu AM, Ting RC, Paran M, Gallo RC (1972) Cordycepin inhibits induction of murine leukovirus production by 5-iodo-2′-deoxyuridine. Proc Natl Acad Sci USA 69: 3820–3824
45. Zieve GN, Roemer EJ (1988) Cordycepin rapidly collapses the intermediate filament networks into juxtanuclear caps in fibroblasts and epidermal cells. Exp Cell Res 177: 19–26
46. Zieve GW, Feeney RJ, Roemer EJ (1987) Cordycepin disrupts the microtubule networks and arrests Nil 8 hamster fibroblasts at the onset of mitosis. Cell Motil Cytoskeleton 7: 337–346